表　IL-1β／IL-1Raバランスにおける I 型IFNs単独またはIL-1β共処置の影響

	細胞名	IFN type	IFN単独		IFN+IL-1β				
			IL-1Ra遺伝子発現変化(a)（無処置群と比較）		IL-1Ra遺伝子発現変化(a)（IL-1β単独処置群と比較）		IL-1β遺伝子発現変化(b)（IL-1β単独処置群と比較）		(a)/(b)
末梢血由来細胞(株)	THP-1	β	↑	7.1 倍	↑	7.3 倍	↓	0.4 倍	–
		α	↑	3.2 倍	↑	2.5 倍	↓	0.5 倍	–
	PBMC	β	↑	115 倍	↑	52 倍	↓	0.02 倍	–
		α	↑	52 倍	↑	27 倍	↓	0.03 倍	–
グリオーマ細胞株	U-251 MG	β	↑	4.5 倍	↑	23 倍	↑	2.1 倍	11
		α	↑	3.3 倍	↑	6.8 倍	↑	2.0 倍	3.4
	A-172	β	↑	14 倍	↑	41 倍	↑	15 倍	2.7
		α	↑	8.7 倍	↑	14 倍	↑	13 倍	1.1

THP-1は100 U/mL、その他は1000 U/mLの天然型IFN-βまたは天然型IFN-αにて12時間処置し、IL-1βの共処置は10ng/mLにてIFNと同時に行った。定法によりtotal RNAを抽出し、逆転写によりcDNAを作製し、IL-1RaおよびIL-1β遺伝子発現レベルをリアルタイムPCR法により解析した。解析にはハウスキーピング遺伝子（GAPDH）の発現量により目的遺伝子の発現量を標準化し、相対定量するΔCt法を用いた。IFN単独処置群は未処置群を、IL-1βとの共処置群はIL-1β単独処置群を対象群として発現変化を算出した。さらにIL-1βとIL-1Ra遺伝子の発現バランスを考察するため、IL-1β共処置群に関してはさらに各遺伝子の発現変化の比を算出した。

ト末梢血細胞およびヒト神経膠（芽）腫細胞株（グリオーマ細胞株）を用いて検討した。また，C型慢性肝炎罹患状態は炎症状態にあるととらえ，炎症性サイトカインの一つであるIL-1β共処置時のIFNの影響についても検討した。

1. IL-1β／IL-1Raバランスにおける IFN単独またはIL-1β共処置の影響（表）

これまでI型IFNsによるIL-1Ra産生の検討によく用いられてきたTHP-1細胞[12]およびPBMC[13]を末梢血由来細胞として，また先述のIFN-αによる中枢でのIL-1β産生細胞がアストログリアであるとされていたこと[7]，ヒト中枢でのIFNによるIL-1Ra産生細胞はミクログリアであるとの報告があることから[14]，ヒトグリオーマ細胞株であるU-251 MG細胞およびA-172細胞を中枢由来の細胞として用いた。各細胞におけるI型IFNs単独またはIL-1β共処置によるIL-1βおよびIL-1Ra遺伝子発現変化をリアルタイムPCR法にて解析し，それぞれの対象群に対する発現変化を表に示した。IFN-αまたはIFN-βの単独あるいはIL-1β共処置により，IL-1Ra遺伝子の発現は増加し，その程度はいずれの細胞においてもIFN-αよりIFN-βの方が大きかった。なお，このIL-1Ra遺伝子発現変化はIFNの濃度依存的であった（データ非提示）。興味深いことに，U-251 MGおよびA-172細胞では，IFN単独に比べてIL-1β存在下において，よりIL-1Ra遺伝子の発現増加が増強される傾向が認められ，さらにその増強の程度はIFN-βによってそれぞれ5倍および3倍，IFN-αによってそれぞれ約2倍と，IFN-βの方が大きかった。すなわち，I型IFNs，特にIFN-βは特定の細胞では炎症下でより抗炎症作用を発揮する可能性が考えられた。

一方，IL-1β処置によりautocrineに増加したIL-1β遺伝子発現は（データ非提示），IFN処置により末梢血由来細胞では抑制され，グリオーマ細胞では増加した。そこでIL-1βとIL-1Ra遺伝子の発現バランスを考察するため，グリオーマ細胞におけるIL-1β共処置時の各遺伝子の発現変化の比を算出したところ，IFN-αもIFN-βもIL-1Ra遺伝子の発現増加の方がIL-1βの発現増加より優っていた。更にその比はIFN-β処置の方が大きかったため，IFN-βはIFN-αよりもIL-1β／IL-1RaバランスをIL-1Ra側（抗炎症）に傾ける作用が強いことが推察された。

2. I型IFNsによるIL-1βおよびIL-1Ra遺伝子発現の経時的変化とIL-1Raたん白産生レベル（図1）

血球由来細胞を用いて，IL-1β存在下におけるI型IFNsによるIL-1βおよびIL-1Ra遺伝子発現変化の経時的変化を検討した。THP-1細胞において，IFN-βおよびIFN-αによるIL-1Ra遺伝子発現増加

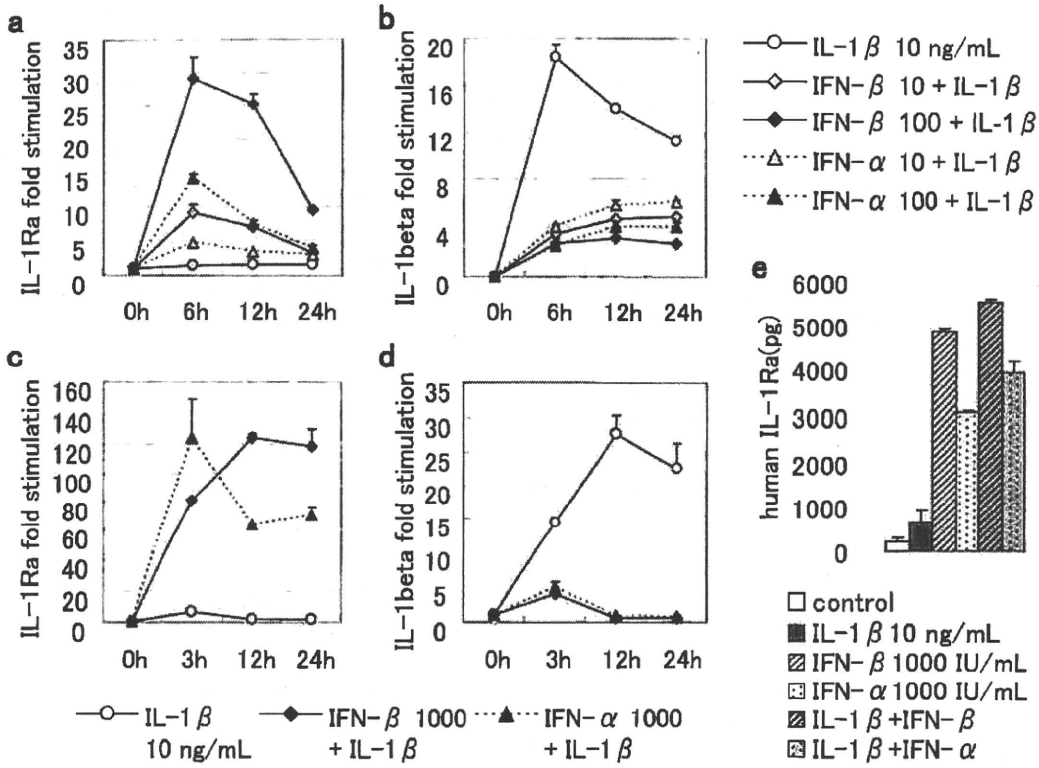

図1　I型IFNsによるIL-1βおよびIL-1Ra遺伝子発現の経時的変化とIL-1Raたん白産生レベル
THP-1細胞（a, b）およびヒトPBMC（c, d, e）は1.5×10⁶ cells/mLにて播種し，THP-1細胞は10または100 U/mL，PBMCは1000 U/mLの天然型IFN-βまたは天然型IFN-αにて所定時間処置した。IL-1βの共処置は10ng/mLにてIFNと同時に行った。遺伝子発現レベルはリアルタイムPCR法にて解析し，各ポイントの無処置群のΔCt値に対する発現比で示した（a, b, c, d）。a, b :THP-1細胞におけるIL-1RaおよびIL-1β遺伝子発現の経時変化，c, d :PBMCにおけるIL-1RaおよびIL-1β遺伝子発現の経時変化，e :24時間処置したPBMCの培養上清中IL-1Raたん白濃度をELISAにて測定。

は6時間でもっとも高く，発現の程度はいずれの測定ポイントでもIFN-αよりIFN-βの方が強かった。また，6時間後と比べ，12時間後のIL-1Ra遺伝子発現レベルはIFN-βよりもIFN-αの方が顕著に低下していた（図1a）。IL-1β処置によるIL-1β遺伝子発現は処置後6時間でもっとも高く，IFN-βおよびIFN-αは濃度依存的にその発現を抑制する傾向を示した（図1b）。ヒトPBMCにおいては，IFN-βによるIL-1Ra遺伝子発現増加は24時間まで低下せず，IFN-αでは3時間をピークに低下した（図1c）。そのため，12時間以降のIL-1Ra遺伝子発現はIFN-αよりもIFN-βの方が高かった。また24時間処置後の培養上清中IL-1Raたん白質濃度は，IFN単独およびIL-1β存在下ともにIFN-αよりもIFN-βの方が高く，遺伝子発現の結果と相関していた（図1e）。一方，IL-1β処置によるIL-1β遺伝子の発現増加は処置後12時間でもっとも高く，IFN-βおよびIFN-αは12時間後以降その発現を完全に抑制した（図1d）。これらのことから，IL-1Ra遺伝子発現レベルにおけるIFN-βとIFN-αの違いには，その発現強度だけでなく，発現亢進の持続性も関与すると考えられる。

おわりに

今回得られた結果をもとに，炎症時（IL-1β存在下）におけるIL-1β／IL-1Ra発現バランスにI型IFNが与える影響を推定図として示した（図2）。末梢（血球由来細胞）では，IL-1β過多により炎症へとバランスが傾くが，I型IFNsはIL-1βの産生を抑制し，さらに内在性アンタゴニストであるIL-1Raの産生を亢進することによって抗炎症作用を示すと考えられる。また，中枢（グリオーマ細胞株）では，I型IFNsはいずれもIL-1βの産生を増加させるが，IL-1β存在下でより増強されるIL-1Raの産生亢進によって，同じく抗炎症作用を発揮することが考えられる。精神神経症状とサイトカインレベルの相関に

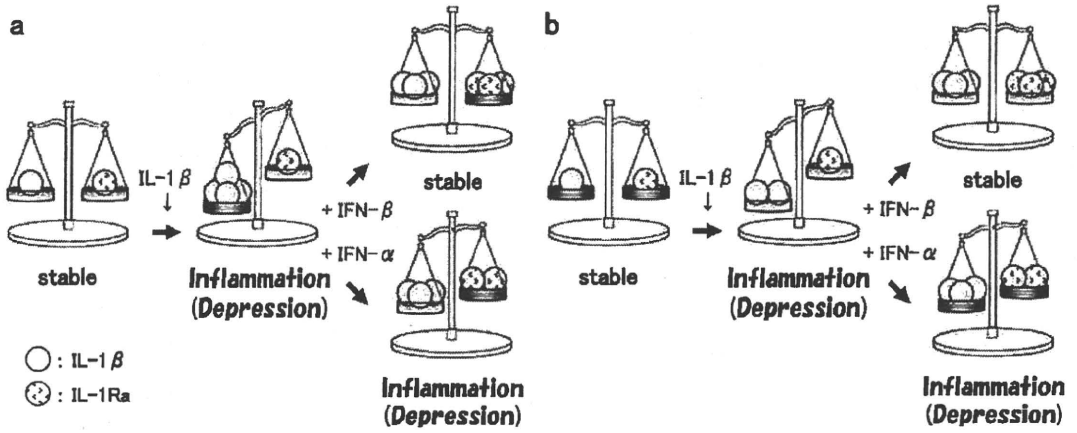

図2　血球系細胞（a）およびグリオーマ細胞（b）におけるIL-1β／IL-1RaバランスへのⅠ型IFNの影響推定図

ついては，末梢と中枢のいずれの報告もあり[15),16)]，どちらが主であるのか，または両者が重要であるのかまだ不明であるが，IFN-βによるIL-1Raの産生亢進がいずれにおいてもIFN-αに比べて強いことが精神神経症状発現頻度の違い[11)]に関与する可能性が考えられた。現在C型慢性肝炎のIFN治療は，血中動態を改善させたポリエチレングリコール化（PEG化）IFNによる週一回の投与が標準となっている。我々は，PEG化したIFN-βとPEG化IFN-αの比較においても，PEG化IFN-βの方がIL-1Ra遺伝子発現の増強作用が強いという結果を得ており，この違いは普遍的なIFN-α／βの違いである可能性が高いと思われた。同じIFN受容体に作用するにもかかわらずIFN-αとIFN-βが生体内に存在する生物学的意義としても注目していきたい。

精神神経症状への他のサイトカインの関与としては，血漿中のIL-6やTNF-α濃度の増加を示唆する報告も多くみられることから[6)]，IFN-βおよびIFN-αによるそれらへの影響とその比較についても興味が持たれるところである。また，IFN-αによる精神神経症状の発現機序については，セロトニントランスポーターの活性化[17)]や，トリプトファン代謝酵素であるindoleamine 2, 3-dioxygenaseの活性化と血中トリプトファンの減少[18)]，直接的なオピオイド作用[19)]などの仮説も提唱されており，今後これらを多角的に検証していくこともIFN-βとIFN-αの精神神経症状をはじめとする薬理作用の差の機序解明に重要であると思われる。

文　献

1) 荒瀬康司．日本臨床. 2004;62: (Suppl 7):519-22.
2) Konsman JP, Parnet P, Dantzer R., Trends Neurosci. 2002;25:154-9.
3) Schiepers OJ, Wichers MC, Maes M., Prog Neuropsychopharmacol Biol Psychiatry. 2005;29:201-17.
4) Maes M., Neuro Endocrinol Lett. 2008;29:287-91.
5) Bluthé RM, Michaud B, Poli V, Dantzer R., Physiol Behav. 2000;70:367-73.
6) Loftis JM, Huckans M, Ruimy S, Hinrichs DJ, Hauser P., Neurosci Lett. 2008;430:264-8.
7) Kaneko N, Kudo K, Mabuchi T, Takemoto K, Fujimaki K, Wati H, Iguchi H, Tezuka H, Kanba S., Neuropsychopharmacology. 2006;31:2619-26.
8) Hayley S, Poulter MO, Merali Z, Anisman H., Neuroscience. 2005;135:659-78.
9) Nicoletti F, Patti F, DiMarco R, Zaccone P, Nicoletti A, Meroni P, Reggio A., Cytokine. 1996;8:395-400.
10) Dionne S, D'Agata ID, Hiscott J, Vanounou T, Seidman EG.., Clin Exp Immunol. 1998;112:435-42.
11) Miller LC, Lynch EA, Isa S, Logan JW, Dinarello CA, Steere AC., Lancet. 1993;341:146-8.
12) Kline JN, Fisher PA, Monick MM, Hunninghake GW., Am J Physiol. 1995;269:L92-8.
13) Coclet-Ninin J, Dayer JM, Burger D., Eur Cytokine Netw. 1997;8:345-9.
14) Liu JS, Amaral TD, Brosnan CF, Lee SC., J Immunol. 1998;161:1989-96.
15) Vollmer-Conna U, Fazou C, Cameron B, Li H, Brennan C, Luck L, Davenport T, Wakefield D, Hickie I, Lloyd A.., Psychol Med. 2004;34:1289-97.
16) Li S, Wang C, Wang W, Dong H, Hou P, Tang Y., Life Sci. 2008;82:934-42.
17) Morikawa O, Sakai N, Obara H, Saito N., Eur J Pharmacol. 1998;349:317-24.
18) Zignego AL, Cozzi A, Carpenedo R, Giannini C, Rosselli M, Biagioli T, Aldinucci A, Laffi G, Moroni F. Dig Liver Dis. 2007;39(Suppl 1):S107-11.
19) Makino M, Kitano Y, Komiyama C, Hirohashi M, Takasuna K. Br J Pharmacol. 2000;130:1269-74.

Industrial Info.

Ⅰ型インターフェロンの肝線維化改善メカニズム

The mechanism of action of type I interferon to improve liver fibrosis

東レ株式会社　医薬研究所

西村　和美・鈴木　知比古

Key words
interferon, liver fibrosis
Hepatic Stellate Cell

要　約

C型慢性肝炎やC型代償性肝硬変に対するインターフェロン（IFN）治療において，ウイルス駆除に至らなくとも，肝線維化の進展や肝癌の発症が抑えられることが示されている。しかし，その詳細な分子機構は不明である。我々は，肝線維化に重要な役割を果たしている肝星細胞（HSC）に対するIFNの直接的作用を明らかにすることを目的として検討を行った。

その結果，Ⅰ型IFNはヒトHSCに対し，①サイクリン依存性キナーゼ阻害因子であるp21の誘導を介して細胞周期のG_1期からS期への移行を抑制し，細胞増殖抑制作用を示すこと，②マトリックスメタロプロテアーゼ（MMP）-1の産生亢進作用およびTGF-βのシグナル抑制作用を示すことを明らかにした。これらのことから，Ⅰ型IFNはHSCに対して直接的に多様な作用を引き起こし，抗線維化作用を示すことが明らかとなった。

はじめに

Ⅰ型インターフェロン（interferon, 以下IFN）は，慢性C型肝炎の治療方法としてウイルス駆除を行う目的で広く用いられている。慢性C型肝炎の治療においては，ウイルス駆除とともに，肝線維化→肝硬変→肝癌への進行をくい止めることが重要である。IFN治療により慢性C型肝炎患者において肝線維化が改善されることは，多数の報告により示されている[1]。しかしながら，IFNによる肝線維化改善作用のメカニズムは明らかにされておらず，一般的にはウイルス排除より肝炎が沈静化した結果による二次的なものであると考えられている。しかし，IFN治療によりC型肝炎ウイルス排除に至らない患者についても，肝線維化の進行が遅延する例があるとの報告[2]があり，IFNによる肝線維化の改善は，ウイルス排除による二次的な機構以外にも，抗線維化メカニズムが存在することが示唆されている。その一候補として，*in vitro*の系において，IFNが細胞外マトリックス産生・分解の中心的な役割を担っている肝星細胞（Hepatic Stellate Cell, 以下HSC）に対して，その増殖や細胞外マトリックスの主要構成成分であるコラーゲンの産生を抑制するとの報告[3]があり，IFNが直接的にHSCに作用して肝線維化を改善する可能性が考えられる。しかし，その詳細なメカニズムは，明らかになっていない。そこで，我々は，ヒトHSC株を用い，Ⅰ型IFNの抗線維化メカニズムを解析した。

1．肝線維化の分子生物学的機構とIFNの作用点（図1）

正常なHSCは，類洞の内皮細胞と肝細胞の間のDisse腔に存在し，pericyteとして類洞の血流の調節を行っていると考えられている。C型肝炎ウイルスなどによる慢性的な肝障害により，肝細胞の一部が，変

Kazumi Nishimura, Tomohiko Suzuki：
Toray Industries, Inc. Pharmaceutical Research Laboratories
〒248-8555　神奈川県鎌倉市手広6丁目10-1　　Tel：0467-32-2111　Fax：0467-32-2135

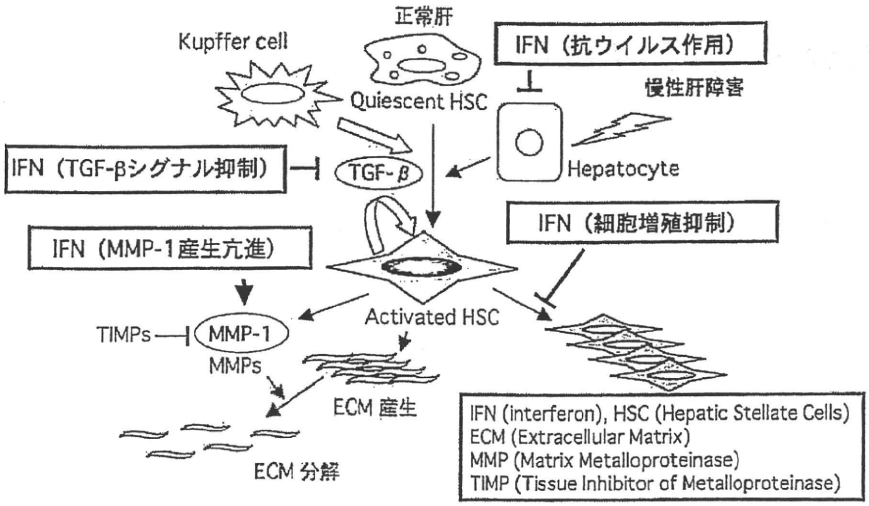

図1　肝線維化の分子生物学的機構とIFNの作用点（文献[4]より引用改変）

性，壊死，アポトーシスに陥ると，マクロファージ系のクッパー細胞が活性化され，TGF-β，PDGFおよびTNF-αなどのサイトカインを放出するようになる。これらのサイトカインによりHSCは活性化され，筋線維芽細胞（myofibroblast）様に形質転換する。活性化されたHSCは自ら増殖し，細胞外マトリックスを産生し，TGF-β，PDGFなどのサイトカインをautocrineで産生し，肝の線維化が進行していく。したがって，HSCの活性を抑制し，細胞外マトリックスの産生を抑えることが肝線維化の治療に有効であると考えられている。HSCの制御をターゲットとした肝線維化阻害剤の研究の例としては，gliotoxin[5]などの細胞毒によるHSCのアポトーシス誘導，コラーゲン分子のシャペロンであるHSP47 siRNAのHSC特異的な導入[6]などの報告があり，動物レベルで有効性が示されている。

IFNの肝線維化抑制における作用点としては，前述のようにC型肝炎ウイルスが感染した肝細胞（hepatocyte）とHSCが考えられる（図1）。IFNは，hepatocyteに作用してウイルスを排除することにより，二次的に肝線維化を改善する。また我々の今回の研究から，IFNはHSCに直接作用し，①細胞増殖を抑制して肝線維化の進行を抑制，②マトリックスメタロプロテアーゼ-Matrix Metalloproteinase-1，以下MMP-1）の産生を促して細胞外マトリックスの分解を促進，③線維化促進因子であるTGF-β シグナルを抑制，することが明らかとなった。

2．HSCに対するⅠ型IFNの細胞増殖および細胞周期への作用

我々が解析したIFNの抗肝線維化メカニズムのひとつとして，まずHSCの増殖抑制作用について詳しく述べる。培養可能なヒトHSC株をヒトⅠ型IFNであるIFN-αあるいはIFN-βで処理し，細胞増殖に対する作用をMTS法にて検討した。また常法により細胞周期に対する作用を解析した。次いで細胞周期に関連するサイクリン依存性キナーゼ（Cyclin Dependent Kinase，以下CDK）阻害因子*p21*遺伝子およびp21蛋白の発現への影響をそれぞれ定量PCR法およびウェスタンブロット法により検討した。

IFN-α またはIFN-β は，HSCに対し細胞増殖抑制作用を示し，同じ生物活性濃度で処置した場合，IFN-βはIFN-α よりも作用が強力であることが明らかとなった（図2a）。IFN-β のHSCの細胞周期に対する作用を解析した結果，IFN-β は，細胞周期のG_0/G_1期からS期への移行を遅らせることで，細胞分裂を抑制することが明らかとなった（図2b）。細胞周期が，G_0/G_1期で停まっていることからCDK阻害因子，特に*p21*遺伝子に着目して定量PCRを行ったところ，IFN-β は*p21*遺伝子の発現を2倍上昇させ(図は示していない)，更に蛋白レベルでもp21の発現を増加させることが確認された（図2c）。一方で他のCDK阻害因子であるp15には影響しないことが示された。

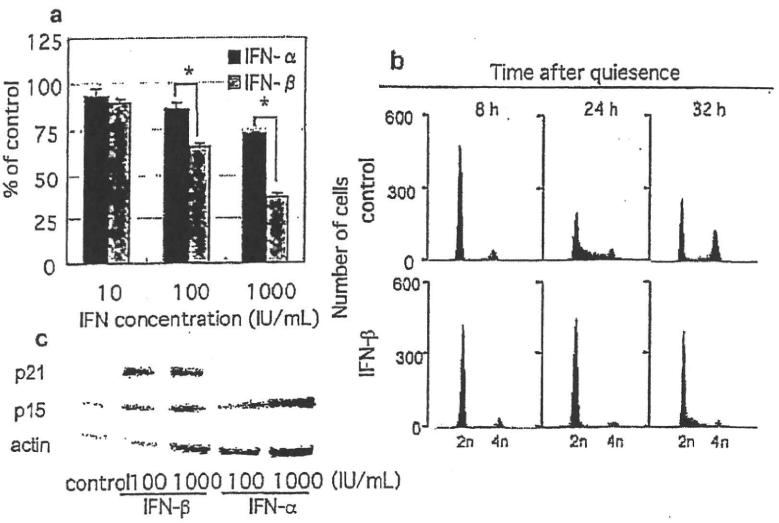

図2　HSCに対するI型IFNの細胞増殖または細胞周期への作用

a：ヒトHSCであるTWNT-4細胞[7]をIFN-βまたはIFN-α 10-1000 IU/mLで処置して5日間培養後，細胞増殖をMTS cell proliferation assayにより測定した。平均値±標準偏差 (n=5)　*p <0.05 (t-test)

b：細胞周期解析は，TWNT-4細胞を無血清培地で培養することによりG_0/G_1期に同調した後，IFN-β 100 IU/mLで処置し，一定時間後にフローサイトメトリーにより細胞内のDNA量を測定した。

c：TWNT-4細胞をIFN-βまたはIFN-α 100，1000 IU/mLで処置して16時間培養後，p21およびp15蛋白の発現をウエスタンブロッティング法により解析した。

3. IFN-βの細胞外マトリックス分解酵素（MMP）に対する作用

HSCは，活性化に伴い細胞外基質を分解するMMPやそれらの阻害因子であるTissue Inhibitor of Metalloproteinase（TIMP）などを産生分泌するようになる。そこで，上述した細胞増殖抑制作用の検討でより強力な作用を示したIFN-β について，ヒトHSC用いて各種*MMP*遺伝子および*TIMP*遺伝子の発現への影響を定量PCR法にて検討した。その結果，IFN-βは*MMP-1*遺伝子の発現を有意に増加させることが明らかとなった（図3a）。有意な変動が認められたMMP-1に注目し，線維化促進因子としての機能が知られているTGF-β 共存下におけるIFN-β の作用を続

a

Gene Name	Time		
	8h	24h	72 h
MMP-1	→	↗1.3folds	↑2 folds
MMP-2	→	→	→
MMP-3	→	→	→
MMP-9	→	→	→
MMP-14	→	→	→
TIMP-1	↗1.2 folds	↗1.2 folds	↗1.3 folds
TIMP-2	→	→	→

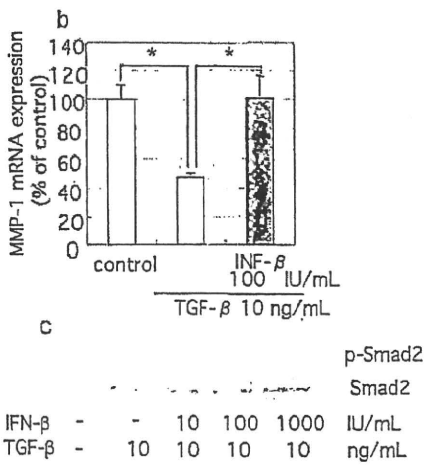

図3　IFN-βの細胞外マトリックス分解酵素（MMP）およびTGF-βシグナルに対する作用

a：ヒトHSCであるLI90細胞[8]をIFN-β 100 IU/mLで処置して一定時間培養後，total RNAを抽出し，MMP-1, -2, -3, -9, -14およびTIMP-1, -2 mRNAの発現レベルをリアルタイムPCR法により定量した。

b：LI90細胞をTGF-β 10 ng/mLとIFN-β 100 IU/mLで同時に処置し，72時間後にMMP-1 mRNAの発現レベルを定量した。平均値±標準偏差 (n=3) *p <0.05 (t-test)

c：LI90細胞をTGF-β 10 ng/mLとIFN-β 10-1000 IU/mLで同時に処置し，24時間後のリン酸化Smad2（p-Smad2）とSmad2蛋白の発現を，ウェスタンブロッティング法により解析した。

いて解析した。TGF-β 処置により *MMP-1* 遺伝子の発現量は低下するが，IFN-β はその発現量を正常レベルにまで回復させることが明らかとなった（図3b）。これら遺伝子レベルでの変動は蛋白レベルでも同様の変化が確認された（図は示していない）。

MMP は細胞外基質の構築や分解に深く関与することが知られており，コラゲナーゼ群（MMP-1, -8, -13），ゼラチナーゼ/IV型コラゲナーゼ群（MMP-2, -9），ストロメライシン群（MMP-3, -10），細胞膜貫通型 MMP 群（MMP-14,-15,-16）に分類される。肝線維症/肝硬変で顕著に増加するのはⅠ型コラーゲンであるので，肝線維化改善には，Ⅰ型コラーゲンを特異的に分解するコラゲナーゼである MMP-1 の発現および活性の調節が重要とされる。このことは，MMP-1 を発現するアデノウイルスベクターを肝硬変ラットに導入することで線維化が抑制されるという報告[9]からも支持され，IFN-β による MMP-1 発現の促進は，その抗線維化メカニズムのひとつとして非常に重要であると考えられる。

MMP-1 に関する上述の検討から，IFN-β が，TGF-β 刺激時のヒト HSC に対して抑制的に働くことが示唆されたため，TGF-β シグナル伝達分子について更に解析を進めた。その結果，HSC において IFN-β 処置により Smad2 のリン酸化が濃度依存的に抑制されることが示された。（図3c）。よって IFN-β による MMP-1 発現の亢進は HSC から autocrine に産生されている TGF-β のシグナルをブロックすることによる作用である可能性が考えられた。

おわりに

Ⅰ型 IFN が動物レベルおよび臨床においても肝線維化を抑制することについては，多くの知見が得られている。また，これまで一方向性と考えられてきた線維化の進行がリバースする可能性があり，Ⅰ型 IFN にその作用を有する可能性が示唆されている[1]。

今回，我々の検討により，Ⅰ型 IFN が，肝線維化において重要な役割を果たしている HSC に対して直接的に，細胞増殖抑制作用，細胞周期抑制作用，MMP-1 産生亢進作用，TGF-β 抑制作用などの多彩な作用を引き起こすことが明らかとなった。現在，我々はⅠ型 IFN を処置した HSC における，高感度 DNA チップ（*3D-Gene*：東レ）を用いた網羅的 miRNA および mRNA の発現解析を実施しており，今後，両結果を関連づけながら詳細な解析を進め，得られた情報からIFN の線維化抑制機構を分子レベルで解明していく予定である。

肝線維化に対するⅠ型 IFN の作用分子機構を詳細に再検討し，明確にすることは，肝線維化を制御する薬物の創薬研究の基盤となり，類似の作用を有する低分子化合物の探索方針を新たに提示する可能性を秘めている。IFN-β や肝線維化に関しては，まだまだ不明な点が多く，新しい手法を用いた細胞分子生物学的なアプローチによって，これらの分子機構を改めて研究しなおすことは非常に意義あることと思われた。

謝辞

ヒト HSC 株 TWNT-4 を提供して下さいました，岡山大学大学院医歯薬学総合研究科消化器・腫瘍外科学の小林直哉先生，および本研究に関して非常に有意義なディスカッションをさせていただきました，九州医療センター消化器科の中牟田誠先生に感謝いたします。

文　献

1) Shiratori Y, *et al.*: Histologic improvement of fibrosis in patients with hepatitis C who have sustained response to interferon therapy. Ann Intern Med. 132 : 517-524, 2000.
2) Alric L, *et al.*: Maintenance therapy with gradual reduction of the interferon dose over one year improves histological response in patients with chronic hepatitis C with biochemical response: results of a randomized trial. J Hepatol. 35 : 272-278, 2001.
3) Mallat A, *et al.*: Interferon alfa and gamma inhibit proliferation and collagen synthesis of human Ito cells in culture. Hepatology 21 : 1003-1010, 1995.
4) 谷口博順ら，インターフェロンの肝線維化抑制機構. 最新医学 55 : 85-88, 2000.
5) Hagens WI, *et al.*: Cellular targeting of the apoptosis-inducing compound gliotoxin to fibrotic rat livers. Journal of Pharmacology and Experimental Therapeutics 324 : 902-910, 2008.
6) Sato Y, *et al.*: Resolution of liver cirrhosis using vitamin A-coupled liposomes to deliver siRNA against a collagen-specific chaperone. Nature Biotechnology 26 : 431-442, 2008.
7) Shibata N, *et al.*: Establishment of an immortalized human hepatic stellate cell line to develop antifibrotic therapies. Cell Transplantation 12 : 499-507, 2003.
8) Murakami K, *et al.*: Establishment of a new human cell line, LI90, exhibiting characteristics of hepatic Ito (fat-storing) cells. Lab Invest 72 : 731-739, 1995.
9) Iimuro Y, *et al.*: Delivery of matrix metalloproteinase-1 attenuates established liver fibrosis in the rat. Gastroenterology 124 : 445-458, 2003.

OPEN ACCESS Freely available online

PLoS one

The Progression of Liver Fibrosis Is Related with Overexpression of the miR-199 and 200 Families

Yoshiki Murakami[1]*, Hidenori Toyoda[2], Masami Tanaka[3], Masahiko Kuroda[3], Yoshinori Harada[4], Fumihiko Matsuda[1], Atsushi Tajima[5¤], Nobuyoshi Kosaka[6], Takahiro Ochiya[6], Kunitada Shimotohno[7]

1 Center for Genomic Medicine, Kyoto University Graduate School of Medicine, Kyoto, Japan, 2 Department of Gastroenterology, Ogaki Municipal Hospital, Ogaki, Japan, 3 Department of Molecular Pathology, Tokyo Medical University, Tokyo, Japan, 4 Department of Pathology and Cell Regulation, Kyoto Prefectural University of Medicine, Kyoto, Japan, 5 Department of Molecular Life Science, Tokai University School of Medicine, Isehara, Japan, 6 Division of Molecular and Cellular Medicine, National Cancer Center Research Institute, Tokyo, Japan, 7 Research Institute, Chiba Institute of Technology, Narashino, Japan

Abstract

Background: Chronic hepatitis C (CH) can develop into liver cirrhosis (LC) and hepatocellular carcinoma (HCC). Liver fibrosis and HCC development are strongly correlated, but there is no effective treatment against fibrosis because the critical mechanism of progression of liver fibrosis is not fully understood. microRNAs (miRNAs) are now essential to the molecular mechanisms of several biological processes. In order to clarify how the aberrant expression of miRNAs participates in development of the liver fibrosis, we analyzed the liver fibrosis in mouse liver fibrosis model and human clinical samples.

Methodology: In a CCL_4-induced mouse liver fibrosis model, we compared the miRNA expression profile from CCL_4 and olive oil administrated liver specimens on 4, 6, and 8 weeks. We also measured expression profiles of human miRNAs in the liver biopsy specimens from 105 CH type C patients without a history of anti-viral therapy.

Principle Findings: Eleven mouse miRNAs were significantly elevated in progressed liver fibrosis relative to control. By using a large amount of human material in CH analysis, we determined the miRNA expression pattern according to the grade of liver fibrosis. We detected several human miRNAs whose expression levels were correlated with the degree of progression of liver fibrosis. In both the mouse and human studies, the expression levels of miR-199a, 199a*, 200a, and 200b were positively and significantly correlated to the progressed liver fibrosis. The expression level of fibrosis related genes in hepatic stellate cells (HSC), were significantly increased by overexpression of these miRNAs.

Conclusion: Four miRNAs are tightly related to the grade of liver fibrosis in both human and mouse was shown. This information may uncover the critical mechanism of progression of liver fibrosis. miRNA expression profiling has potential for diagnostic and therapeutic applications.

Citation: Murakami Y, Toyoda H, Tanaka M, Kuroda M, Harada Y, et al. (2011) The Progression of Liver Fibrosis Is Related with Overexpression of the miR-199 and 200 Families. PLoS ONE 6(1): e16081. doi:10.1371/journal.pone.0016081

Editor: Chad Creighton, Baylor College of Medicine, United States of America

Received September 15, 2010; **Accepted** December 6, 2010; **Published** January 24, 2011

Funding: This work was supported by the Japanese Ministry of Health, Labour and Welfare (Y.M, and K.S). This work was also supported by the 'Strategic Research-Based Support' Project for private universities; with matching funds from the Ministry of Education, Culture, Sports, Science and Technology (M.K). The funders had no role in study design, data collection and analysis, decision to publish, or preparation of the manuscript.

Competing Interests: The authors have declared that no competing interests exist.

* E-mail: ymurakami@genome.med.kyoto-u.ac.jp

¤ Current address: Department of Human Genetics and Public Health, Institute of Health Biosciences, The University of Tokushima Graduate School, Tokushima, Japan

Introduction

Chronic viral hepatitis is a major risk factor for hepatocellular carcinoma (HCC) [1]. Worldwide 120–170 million persons are currently chronically Hepatitis C Virus (HCV) infected [2]. Due to repetitive and continuous inflammation, these patients are at increased risk of developing cirrhosis, subsequent liver decompensation and/or hepatocellular carcinoma. However, the current standard of care; pegylated interferon and rivabirin combination therapy is unsatisfied in the patients with high titre of HCVRNA and genotype 1b. Activated human liver stellate cells (HSC) with chronic viral infection, can play a pivotal role in the progression of liver fibrosis [3]. Activated HSC produce a number of profibrotic cytokines and growth factors that perpetuate the fibrotic process through paracrine and autocrine effects.

MicroRNAs (miRNAs) are endogenous small non-coding RNAs that control gene expression by degrading target mRNA or suppressing their translation [4]. There are currently 940 identifiable human miRNAs (The miRBase Sequence Database - Release ver. 15.0). miRNAs can recognize hundreds of target genes with incomplete complementary; over one third of human genes appear to be conserved miRNA targets [5][6]. miRNA is associated several pathophysiologic events as well as fundamental cellular processes such as cell proliferation and differentiation. Aberrant expression of miRNA can be associated with the liver diseases [7][8][9][10]. Recently reported miRNAs can regulate the activation of HSCs and thereby regulate liver fibrosis. miR-29b, a negative regulator for the type I collagen and SP1, is a key regulator of liver fibrosis [11]. miR-27a and 27b allowed culture-activated rat HSCs to switch to a more quiescent HSC phenotype,

with restored cytoplasmic lipid droplets and decreased cell proliferation [12].

In this study, we aimed to reveal the association between miRNA expression patterns and the progression of liver fibrosis by using a chronic liver inflammation model in mouse. We also sought to identify the miRNA expression profile in chronic hepatitis (CH) C patients according to the degree of liver fibrosis, and to clarify how miRNAs contribute to the progression of liver fibrosis. We observed a characteristic miRNA expression profile common to both human liver biopsy specimens and mouse CCL_4 specimens, comprising the key miRNAs which are associated with the liver fibrosis. This information is expected to uncover the mechanism of liver fibrosis and to provide a clearer biomarker for diagnosis of liver fibrosis as well as to aid in the development of more effective and safer therapeutic strategies for liver fibrosis.

Results

The expression level of several mouse miRNAs was increased by introducing mouse liver fibrosis

In order to identify changes in the miRNA expression profile between advanced liver fibrosis and non-fibrotic liver, we intraperitoneally administered CCL_4 in olive oil or olive oil alone twice a week for 4 weeks and then once a week for the next 4 weeks. Mice were sacrificed at 4, 6, or 8 weeks and then the degree of mouse liver fibrosis was determined by microscopy (Figure S1). miRNA expression analysis was performed from the liver tissue collected at the same time. Histological examination revealed that the degree of liver fibrosis progressed in mice that received CCL_4 relative to mice receiving olive oil alone (Figure 1A). Microarray analysis revealed that in CCL_4 mice, the expression level of 11 miRNAs was consistently higher than that in control mice (Figure 1B).

miRNA expression profile in each human liver fibrosis grade

We then established human miRNAs expression profile by using 105 fresh-frozen human chronic hepatitis (CH) C liver tissues without a history of anti-viral therapy, classified according to the grade of the liver fibrosis (F0, F1, F2, and F3 referred to METAVIR fibrosis stages)(Figure 2, Table S2). Fibrosis grade F0 was considered to be the negative control because these samples were derived from patients with no finding of liver fibrosis. In zebrafish, most highly tissue-specific miRNAs are expressed during embryonic development; approximately 30% of all miRNAs are expressed at a given time point in a given tissue [13]. In mammals, the 20–30% miRNA call rate has recently been validated [14]. Such analysis revealed that the diversity of miRNA expression level among specimens was small. Therefore, we focused on miRNAs with a fold change in mean expression level greater than 1.5 ($p<0.05$) in the two arbitrary groups of liver fibrosis.

Expression of several miRNAs was dramatically different among grades of fibrosis. In the mice study 11 miRNAs were related to the progression of liver fibrosis (mmu-let-7e, miR-125-5p, 199a-5p, 199b, 199b*, 200a, 200b, 31, 34a, 497, and 802). In the human study 10 miRNAs were extracted, and the change in their expression level varied significantly between F0 and F3 (F0<F3: hsa-miR-146b, 199a, 199a*, 200a, 200b, 34a, and 34b, F0>F3: hsa-miR-212, 23b, and 422b). The expression level of 6 miRNAs was significantly different between F0 and F2 (F0<F2: hsa-miR-146b, 200a, 34a, and 34b, F0>F2: hsa-miR-122 and 23b). 5 extracted miRNAs had an expression level that was significantly different between F1 and F2 (F1<F2: hsa-miR-146b, F1>F2: hsa-miR-122, 197, 574, and 768-5p). The expression level of 9 miRNAs changed significantly between F1 and F3 (F1<F3: hsa-miR-146b, 150, 199a, 199a*, 200a, and 200b, F1>F3: hsa-miR-378, 422b, and 768-5p). The miRNAs related to liver fibrosis were extracted using two criteria: similar expression pattern in both the human and the mice specimens and shared sequence between human and mouse. We compared the sequences of mouse miRNAs as described on the Agilent Mouse MiRNA array Version 1.0 (miRbase Version 10.1) and human miRNAs as described on the Agilent Human MiRNA array Version 1.5 (miRbase Version 9.1). The sequences of mmu-miR-199a-5p, mmu-miR-199b, mmu-miR-199b, mmu-miR-200a, and mmu-miR-200b in mouse miRNA corresponded to the sequences of hsa-miR-199a, hsa-miR-199a*, hsa-miR-199a, hsa-miR-200a, and hsa-miR-200b in human miRNA, respectively (Table S3).

Validation of the microarray result by real-time qPCR

The 4 human miRNAs (miR-199a, miR-199a*, miR-200a, and miR-200b) with the largest difference in fold change between the F1 and F3 groups were chosen to validate the microarray results using stem-loop based real-time qPCR. The result of real-time qPCR supported the result of that microarray analysis. The expression level of these 4 miRNAs was significantly different between F0 and F3 and spearman correlation analysis also showed that the expressions of these miRNAs were strongly and positively correlated with fibrosis grade ($n = 105$, $r = 0.498$(miR-199a), 0.607(miR-199a*), 0.639(miR-200a), 0.618(miR-200b), p-values<0.0001) (Figure 3).

Over expression of miR-199a, 199a*, 200a, and 200b was associated with the progression of liver fibrosis

In order to reveal the function of miR-199a, miR-199a*, miR-200a, and miR-200b, we investigated the involvement of these miRNAs in the modulation of fibrosis-related gene in LX-2 cells. The endogenous expression level of these 4 miRNAs in LX2 and normal liver was low according to the microarray study (Figure S2). Transforming growth factor (TGF)β is one of the critical factors for the activation of HSC during chronic inflammation [15] and TGFβ strongly induced expression of three fibrosis-related genes include a matrix degrading complex comprised of α1 procollagen, matrix remodeling complex, comprised of metalloproteinases-13 (MMP-13), tissue inhibitors of metalloproteinases-1 (TIMP-1) in LX-2 cells (Figure 4A). Furthermore, overexpression of miR-199a, miR-199a*, miR-200a and miR-200b in LX-2 cells resulted significant induction of above fibrosis-related genes compared with control miRNA (Figure 4B). Finally we validated the involvement of TGFβ in the modulation of these miRNAs. In LX-2 cells treated with TGFβ, the expression levels of miR-199a and miR-199a* were significantly higher than in untreated cells; the expression levels of miR-200a and miR-200b were significantly lower than in untreated cells. Thus, our in vitro analysis suggested a possible involvement of miR-199a, 199a*, 200a, and 200b in the progression of liver fibrosis.

Discussion

Our comprehensive analysis showed that the aberrant expression of miRNAs was associated with the progression of liver fibrosis. We identified that 4 highly expressed miRNAs (miR-199a, miR-199a*, miR-200a, and miR-200b) that were significantly associated with the progression of liver fibrosis both human and mouse. Coordination of aberrant expression of these miRNAs may contribute to the progression of liver fibrosis.

Prior studies have discussed the expression pattern of miRNA found in liver fibrosis samples between previous and present study. In this report and prior mouse studies and the expression pattern of

A

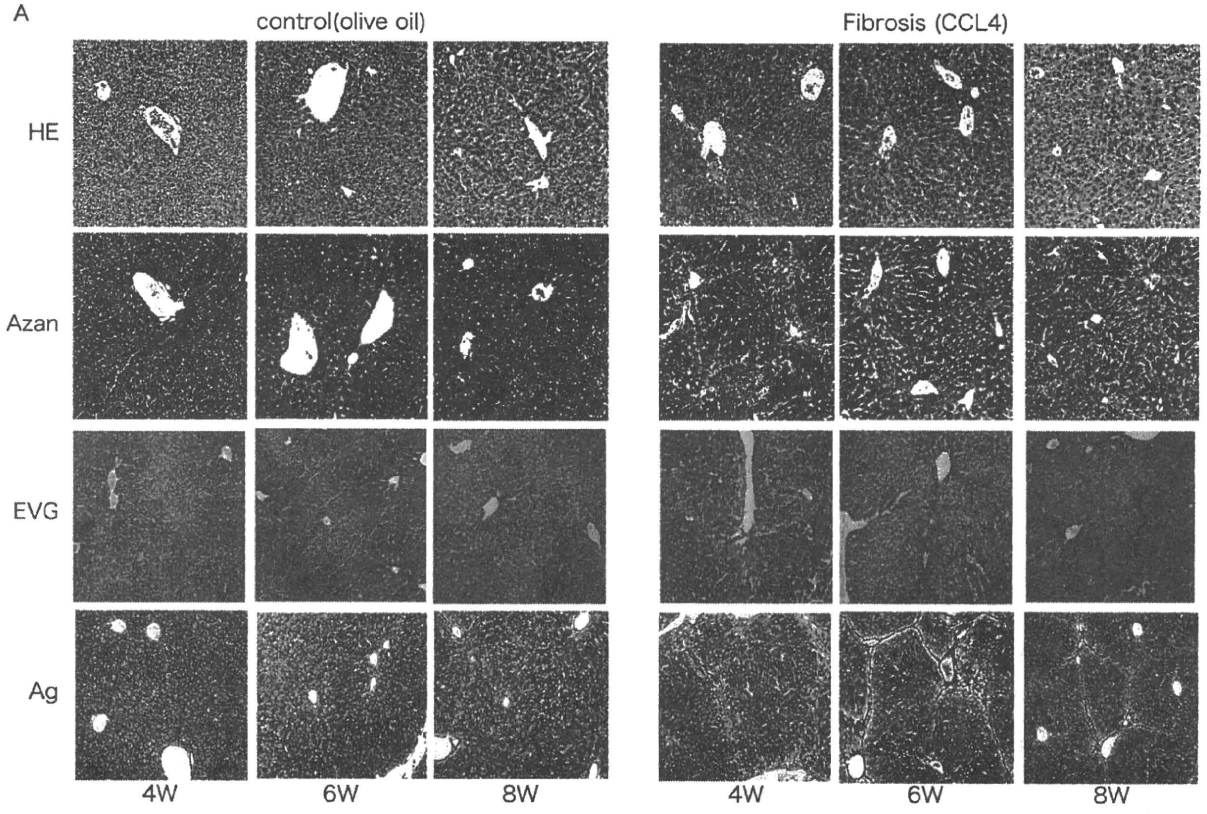

B

miRNA	Fold change CCL4 mouse/control		
	4week	6week	8week
mmu-let-7e	2.92	2.09	2.64
mmu-miR-125a-5p	4.29	2.35	2.67
mmu-miR-199a-5p	2.71	2.12	2.38
mmu-miR-199b	3.25	2.55	2.49
mmu-miR-199b*	5.13	4.47	3.94
mmu-miR-200a	2.23	1.63	2.02
mmu-miR-200b	2.38	2.06	2.20
mmu-miR-31	3.4	2.35	3.19
mmu-miR-34a	3.89	3.22	3.5
mmu-miR-497	2.25	2.00	2.55
mmu-miR-802	2.02	2.87	2.74

Figure 1. The change of liver fibrosis in mouse model. A. Representative H&E-stained, Azan-stained, Ag-stained, and EVG-stained histological sections of liver from mice receiving olive oil alone or CCL_4 in olive oil. Magnification is ×10. B. The expression level of mmu-miRNA in mouse liver with olive oil or CCL_4 at 4W, 6W, and 8W respectively, by microarray analysis.
doi:10.1371/journal.pone.0016081.g001

3 miRNAs (miR-199a-5p, 199b*, 125-5p) was found to be similar while the expression pattern of 11 miRNAs (miR-223, 221, 24, 877, 29b, 29a, 29c, 30c, 365, 148a, and 193) was partially consistent with fibrosis grade [16]. In low graded liver fibrosis, the low expression pattern of 3 miRNAs (miR-140, 27a, and 27b) and the high expression pattern of 6 miRNAs in rat miRNAs (miR-29c*, 143, 872, 193, 122, and 146) in rat miRNA was also similar to our mouse study (GEO Series accession number GSE19865) [11] [12] [17].

The results in this study and previously completed human studies reveal that the expression level of miR-195, 222, 200c, 21, and let-7d was higher in high graded fibrotic liver tissue than in low graded fibrotic liver tissue. Additionally, the expression level of miR-301, 194, and 122 was lower in the high graded fibrotic liver tissue than in low graded fibrotic liver tissue [18] [19] [20](GEO Series accession number GSE16922). This difference in miRNA expression pattern may be contributed to (1) the difference of microarray platform, (2) difference of analytic procedure, and (3) the difference of the species (rat, mouse, and human).

The miR-199 and miR-200 families have are circumstantially related to liver fibrosis. TGFβ-induced factor (TGIF) and SMAD

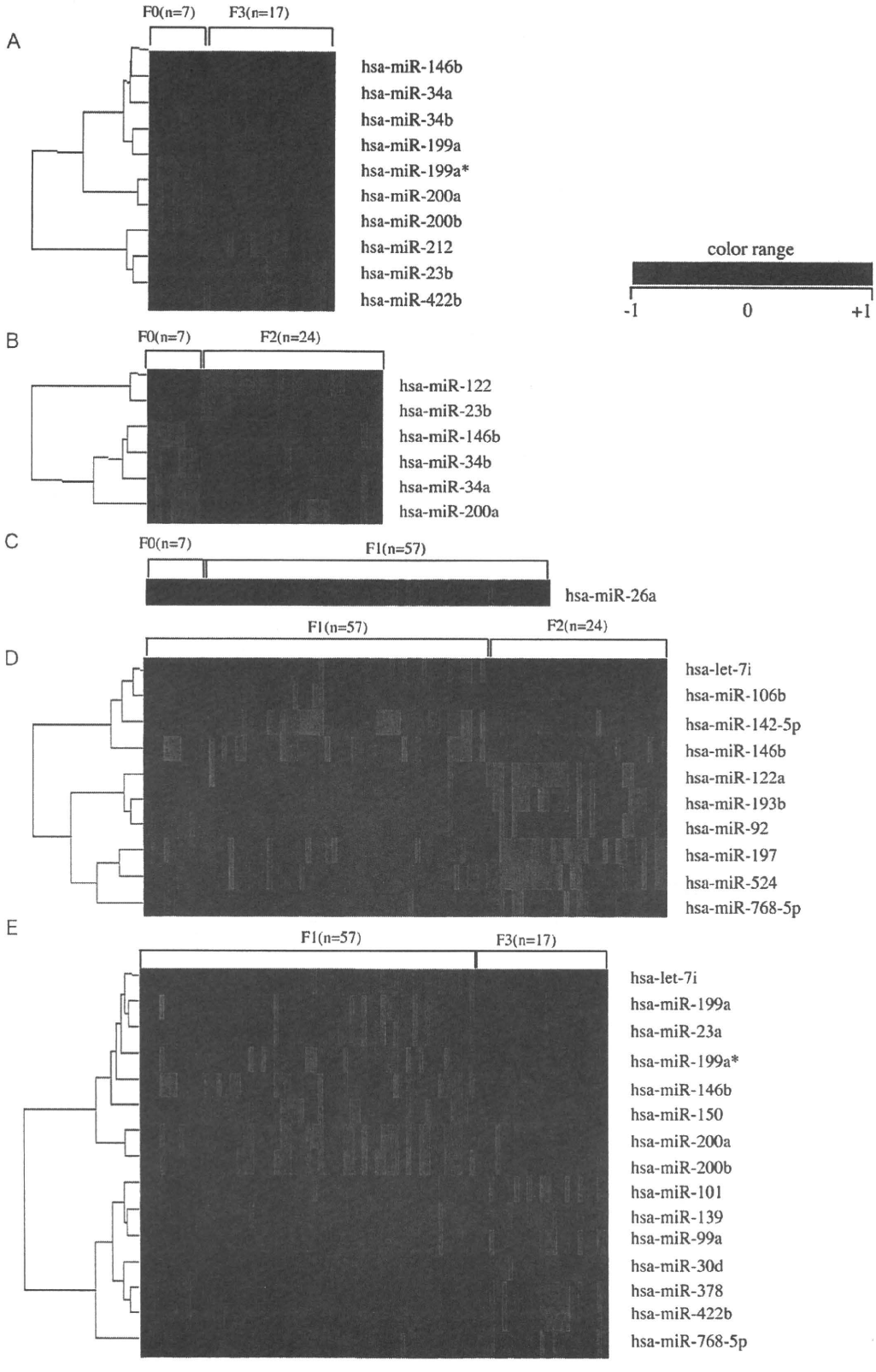
A
F0(n=7)
F3(n=17)
hsa-miR-146b
hsa-miR-34a
hsa-miR-34b
hsa-miR-199a
hsa-miR-199a*
hsa-miR-200a
hsa-miR-200b
hsa-miR-212
hsa-miR-23b
hsa-miR-422b
color range
-1
0
+1
B
F0(n=7)
F2(n=24)
hsa-miR-122
hsa-miR-23b
hsa-miR-146b
hsa-miR-34b
hsa-miR-34a
hsa-miR-200a
C
F0(n=7)
F1(n=57)
hsa-miR-26a
D
F1(n=57)
F2(n=24)
hsa-let-7i
hsa-miR-106b
hsa-miR-142-5p
hsa-miR-146b
hsa-miR-122a
hsa-miR-193b
hsa-miR-92
hsa-miR-197
hsa-miR-524
hsa-miR-768-5p
E
F1(n=57)
F3(n=17)
hsa-let-7i
hsa-miR-199a
hsa-miR-23a
hsa-miR-199a*
hsa-miR-146b
hsa-miR-150
hsa-miR-200a
hsa-miR-200b
hsa-miR-101
hsa-miR-139
hsa-miR-99a
hsa-miR-30d
hsa-miR-378
hsa-miR-422b
hsa-miR-768-5p

Figure 2. Liver fibrosis in human liver biopsy specimen. A. B. C. D. and E. miRNAs whose expression differs significantly between F0 and F3, F0 and F1, F0 and F2, F1 and F2, and F1 and F3, respectively. Relative expression level of each miRNA in human liver biopsy specimen by microarray. Data from microarray were also statistically analyzed using Welch's test and the Bonferroni correction for multiple hypotheses testing. Fold change, p-value are listed in Table S2.
doi:10.1371/journal.pone.0016081.g002

specific E3 ubiquitin protein ligase 2 (SMURF2), both of which play roles in the TGFβ signaling pathway, are candidate targets of miR-199a* and miR-200b, respectively, as determined by the Targetscan algorithm. The expression of miR-199a* was silenced in several proliferating cell lines excluding fibroblasts [21]. Down regulation of miR-199a, miR-199a* and 200a in chronic liver injury tissue was associated with the hepatocarcinogenesis [9]. miR-199a* is also one of the negative regulators of the HCV replication [22]. According to three target search algorithms (Pictar, miRanda, and Targetscan), the miRNAs that may be associated with the liver fibrosis can regulate several fibrosis-related genes (Table S4). Aberrant expression of these miRNAs may be closely related to the progress of the chronic liver disease.

Epithelial-mesenchymal transition (EMT) describes a reversible series of events during which an epithelial cell loses cell-cell contacts and acquires mesenchymal characteristics [23]. Although EMT is not a common event in adults, this process has been implicated in such instances as wound healing and fibrosis. Recent reports showed that the miR-200 family regulated EMT by targeting EMT accelerator ZEB1 and SIP1 [24]. From our observations, overexpression of miR-200a and miR-200b can be connected to the progression of liver fibrosis.

The diagnosis and quantification of fibrosis have traditionally relied on liver biopsy, and this is still true at present. However, there are a number of drawbacks to biopsy, including the invasive nature of the procedure and inter-observer variability. A number of staging systems have been developed to reduce both the inter-observer variability and intra-observer variability, including the METAVIR, the Knodell fibrosis score, and the Scheuer score. However, the reproducibility of hepatic fibrosis and inflammatory activity is not as consistent [25]. In fact, in our study, the degree of fibrosis of the two arbitrary fibrosis groups was classified using the miRNA expression profile with 80% or greater accuracy (data not shown). Thus, miRNA expression can be used for diagnosis of liver fibrosis.

In this study we investigated whether common miRNAs in human and mouse could influence the progression of the liver fibrosis. The signature of miRNAs expression can also serves as a tool for understanding and investigating the mechanism of the onset and progression of liver fibrosis. The miRNA expression profile has the potential to be a novel biomarker of liver fibrosis.

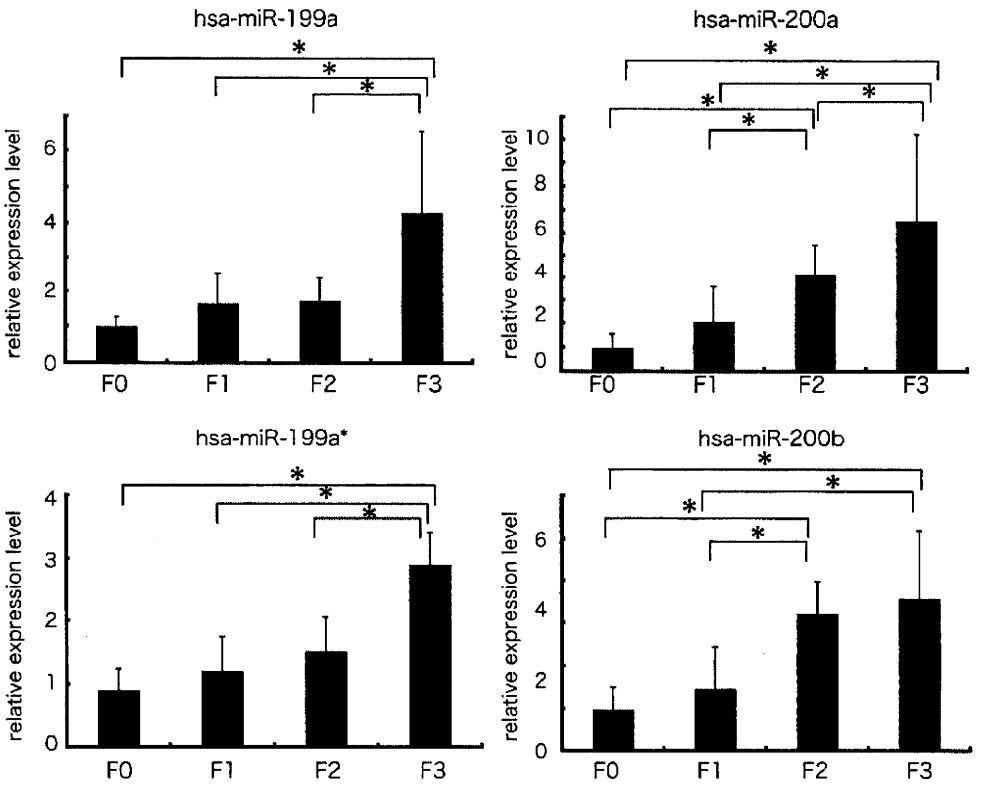

Figure 3. The expression level of miR-199 and 200 families in human liver biopsy specimen by real-time qPCR. Real-time qPCR validation of the 4 miRNAs (miR-199a, miR-199a*, miR-200a, and miR-200b). Each column represents the relative amount of miRNAs normalized to the expression level of U18. The data shown are the means+SD of three independent experiments. Asterisks indicates to a significant difference of $p<0.05$ (two-tailed Student-t test), respectively.
doi:10.1371/journal.pone.0016081.g003

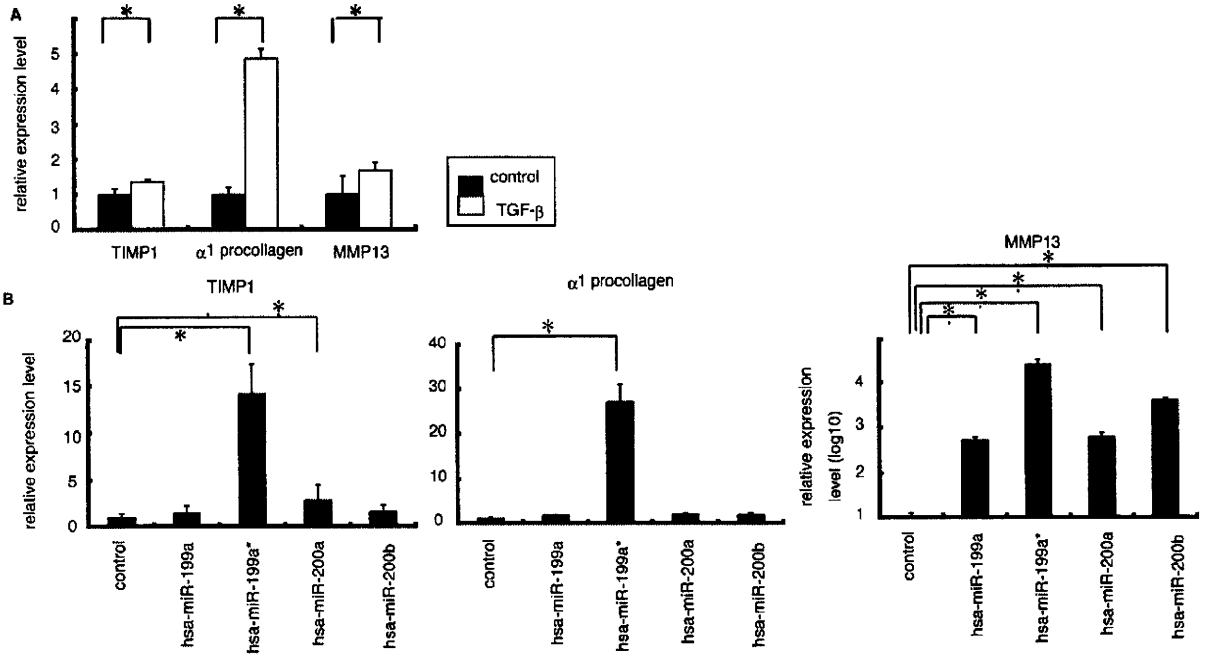

Figure 4. The relationship between expression level of miR-199 and 200 families and expression level of three fibrosis related genes. A. Administration of TGFβ in LX2 cells showed that the expression level of three fibrosis related genes were higher than that in non-treated cells. The data shown are the means+SD of three independent experiments. Asterisk was indicated to the significant difference of $p<0.05$ (two-tailed Student-t test). B. The expression levels of 3 fibrosis related genes in LX2 cells with overexpressing miR-199a, 199a*, 200a, or 200b, respectively were significantly higher than that in cells transfected with control miRNA ($p<0.05$; two-tailed Student t-test).
doi:10.1371/journal.pone.0016081.g004

Moreover miRNA expression profiling has further applications in novel anti-fibrosis therapy in CH.

Materials and Methods

Sample preparation

105 liver tissues samples from chronic hepatitis C patients (genotype 1b) were obtained by fine needle biopsy (Table S1). METAVIR fibrosis stages were F0 in 7 patients, F1 in 57, F2 in 24 and F3 in 17. Patients with autoimmune hepatitis or alcoholic liver injury were excluded. None of the patients were positive for hepatitis B virus associated antigen/ antibody or anti human immunodeficiency virus antibody. No patient received interferon therapy or immunomodulatory therapy prior to the enrollment in this study. We also obtained normal liver tissue from the Liver Transplantation Unit of Kyoto University. All of the patients or their guardians provided written informed consent, and Kyoto University Graduate School and Faculty of Medicine's Ethics Committee approved all aspects of this study in accordance with the Helsinki Declaration.

RNA preparation and miRNA microarray

Total RNA from cell lines or tissue samples was prepared using a *mir*Vana miRNA extraction Kit (Ambion, Austin, TX, USA) according to the manufacturer's instruction. miRNA microarrays were manufactured by Agilent Technologies (Santa Clara, CA, USA) and 100 ng of total RNA was labeled and hybridized using the Human microRNA Microarray Kit protocol for use with Agilent microRNA microarrays Version 1.5 and Mouse microRNA Microarray Kit protocol for use with Agilent microRNA microarrays Version 1.0. Hybridization signals were detected with a DNA microarray scanner G2505B (Agilent Technologies) and the scanned images were analyzed using Agilent feature extraction software (v9.5.3.1). Data were analyzed using GeneSpring GX 7.3.1 software (Agilent Technologies) and normalized as follows: (i) Values below 0.01 were set to 0.01. (ii) In order to compare between one-color expression profile, each measurement was divided by the 75th percentile of all measurements from the same species. The data presented in this manuscript have been deposited in NCBI's Gene Expression Omnibus and are accessible through GEO Series accession number GSE16922 (human) and accession number GSE19865 (mouse).

Real-time qPCR for human miRNA

For detection of the miRNA level by real-time qPCR, TaqMan® microRNA assay (Applied Biosystems) was used to quantify the relative expression level of miR-199a (assay ID. 002304), miR-199a* (assay ID. 000499), miR-200a (assay ID. 000502), miR-200b (assay ID. 002251), and U18 (assay ID. 001204) was used as an internal control. cDNA was synthesized using the Taqman miRNA RT Kit (Applied Biosystems). Total RNA (10 ng/ml) in 5ml of nuclease free water was added to 3 ml of 5× RT primer, 10× 1.5μl of reverse transcriptase buffer, 0.15 μl of 100 mM dNTP, 0.19 μl of RNase inhibitor, 4.16 μl of nuclease free water, and 50U of reverse transcriptase in a total volume of 15 μl. The reaction was performed for 30 min at 16°C, 30 min at 42°C, and 5 min at 85°C. All reactions were run in triplicate. Chromo 4 detector (BIO-RAD) was used to detect miRNA expression.

Animal and Chronic Mouse Liver Injury Model

Each 5 adult (8-week-old) male C57BL/6J mice were given a biweekly intra-peritoneal dose of a 10% solution of CCl_4 in olive oil (0.02 ml/g/ mouse) for the first 4 weeks and then once a week

for the next 4 weeks. At week 4, 6 or 8, the mice were sacrificed. Partial livers were fixed, embedded in paraffin, and processed for histology. Serial liver sections were stained with hematoxylin-eosin, Azan staining, Silver (Ag) staining, and Elastica van Gieson (EVG) staining, respectively. Total RNA from mice liver tissue was prepared as described previously. All animal procedures concerning the analysis of liver injury were performed in following the guidelines of the Kyoto University Animal Research Committee and were approved by the Ethical Committee of the Faculty of Medicine, Kyoto University.

Cell lines and Cell preparation

The human stellate cell lines LX-2, was provided by Scott L. Friedman. LX-2 cells, which viable in serum free media and have high transfectability, were established from human HSC lines [26]. LX-2 cells were maintained in D-MEM (Invitrogen, Carlsbad, CA, USA) with 10% fetal bovine serum, plated in 60 mm diameter dishes and cultured to 70% confluence. Huh-7 and Hela cells were also maintained in D-MEM with 10% fetal bovine serum. HuS-E/2 immortalized hepatocytes were cultured as described previously [27]. LX-2 cells were then cultured in D-MEM without serum with 0.2% BSA for 48 hours prior to TGFβ1 (Sigma-Aldrich, Suffolk, UK) treatment (2.5 ng/ml for 20 hours). Control cells were cultured in D-MEM without fetal bovine serum.

miRNA transfection

LX-2 cells were plated in 6-well plates the day before transfection and grown to 70% confluence. Cells were transfected with 50 pmol of Silencer® negative control siRNA (Ambion) or double-stranded mature miRNA (Hokkaido System Science, Sapporo, Japan) using lipofectamine RNAiMAX (Invitrogen). Cells were harvested 2 days after transfection.

Real-time qPCR

cDNA was synthesized using the Transcriptor High Fiderity cDNA synthesis Kit (Roche, Basel, Switzerland). Total RNA (2 μg) in 10.4 μl of nuclease free water was added to 1 μl of 50mM random hexamer. The denaturing reaction was performed for 10min at 65°C. The denatured RNA mixture was added to 4 μl of 5× reverse transcriptase buffer, 2 μl of 10 mM dNTP, 0.5 μl of 40U/μl RNase inhibitor, and 1.1 μl of reverse transcriptase (FastStart Universal SYBR Green Master (Roche) in a total volume of 20 μl. The reaction ran for 30 min at 50°C (cDNA synthesis), and five min at 85°C (enzyme denaturation). All reactions were run in triplicate. Chromo 4 detector (BIO-RAD, Hercules, CA, USA) was used to detect mRNA expression. The primer sequences are follows; MMP13 s; 5′-gaggctccgagaaatgcagt-3′, as; 5′-atgccatcgtgaagtctggt-3′, TIMP1 s; 5′-cttggcttctgcactgatgg-3′, as; 5′-acgctggtataaggtggtct-3′, α1-procollagen s; 5′-aacatgaccaaaaaccaaaagtg-3′, as; 5′-cattgtttcctgtgtcttctgg-3′, and β-actin s; 5′-ccactggcatcgtgatggac-3′, as; 5′-tcattgccaatggtgatgacct-3′. Assays were performed in triplicate, and the expression levels of target genes were normalized to expression of the β-actin gene, as quantified using real-time qPCR as internal controls.

Statistical analyses

Statistical analyses were performed using Student's *t*-test; *p* values less than 0.05 were considered statistically significant. Microarray data were also statistically analyzed using Welch's test and Bonferroni correction for multiple hypotheses testing.

Supporting Information

Figure S1 Time line of the induction of chronic liver fibrosis. Upward arrow indicated administration of olive oil or CCl_4. Downward arrow indicates when mice were sacrificed.
(TIF)

Figure S2 Comparison of the expression level of miR-199 and 200 familes in several cell lines and human liver tissue. Endogenous expression level of miR-199a, 199a*, 200a, and 200b in normal liver and LX2 cell as determined by microarray analysis (Agilent Technologies). Endogenous expression level of same miRNAs in Hela, Huh-7 and, immortalized hepatocyte: HuS-E/2 by previously analyzed data [9].
(TIF)

Table S1 Clinical characteristics of patients by the grade of fibrosis.
(DOCX)

Table S2 Extracted human miRNAs related to liver fibrosis.
(DOCX)

Table S3 Corresponding human and mouse miRNAs.
(DOCX)

Table S4 Hypothetical miRNA target genes according to in silico analysis.
(DOCX)

Author Contributions

Conceived and designed the experiments: YM KS. Performed the experiments: YM HT YH NK. Analyzed the data: MT MK. Contributed reagents/materials/analysis tools: YM HT YH NK. Wrote the paper: YM MT AT FM NK TO.

References

1. Wasley A, Alter MJ (2000) Epidemiology of hepatitis C: geographic differences and temporal trends. Semin Liver Dis 20: 1–16.
2. Shepard CW, Finelli L, Alter MJ (2005) Global epidemiology of hepatitis C virus infection. Lancet Infect Dis 5: 558–567.
3. Gressner AM, Weiskirchen R (2006) Modern pathogenetic concepts of liver fibrosis suggest stellate cells and TGF-beta as major players and therapeutic targets. J Cell Mol Med 10: 76–99.
4. Nilsen TW (2007) Mechanisms of microRNA-mediated gene regulation in animal cells. Trends Genet 23: 243–249.
5. Zamore PD, Haley B (2005) Ribo-gnome: the big world of small RNAs. Science 309: 1519–1524.
6. Pillai RS (2005) MicroRNA function: multiple mechanisms for a tiny RNA? Rna 11: 1753–1761.
7. Ura S, Honda M, Yamashita T, Ueda T, Takatori H, et al. (2009) Differential microRNA expression between hepatitis B and hepatitis C leading disease progression to hepatocellular carcinoma. Hepatology 49: 1098–1112.
8. Yamamoto Y, Kosaka N, Tanaka M, Koizumi F, Kanai Y, et al. (2009) MicroRNA-500 as a potential diagnostic marker for hepatocellular carcinoma. Biomarkers 14: 529–538.
9. Murakami Y, Yasuda T, Saigo K, Urashima T, Toyoda H, et al. (2006) Comprehensive analysis of microRNA expression patterns in hepatocellular carcinoma and non-tumorous tissues. Oncogene 25: 2537–2545.
10. Jin X, Ye YF, Chen SH, Yu CH, Liu J, et al. (2008) MicroRNA expression pattern in different stages of nonalcoholic fatty liver disease. Dig Liver Dis.
11. Ogawa T, Iizuka M, Sekiya Y, Yoshizato K, Ikeda K, et al. (2009) Suppression of type I collagen production by microRNA-29b in cultured human stellate cells. Biochem Biophys Res Commun.
12. Ji J, Zhang J, Huang G, Qian J, Wang X, et al. (2009) Over-expressed microRNA-27a and 27b influence fat accumulation and cell proliferation during rat hepatic stellate cell activation. FEBS Lett 583: 759–766.
13. Wienholds E, Kloosterman WP, Miska E, Alvarez-Saavedra E, Berezikov E, et al. (2005) MicroRNA expression in zebrafish embryonic development. Science 309: 310–311.

14. Landgraf P, Rusu M, Sheridan R, Sewer A, Iovino N, et al. (2007) A mammalian microRNA expression atlas based on small RNA library sequencing. Cell 129: 1401–1414.
15. Friedman SL (2008) Hepatic fibrosis-Overview. Toxicology.
16. Roderburg C, Urban GW, Bettermann K, Vucur M, Zimmermann H, et al. (2010) Micro-RNA profiling reveals a role for miR-29 in human and murine liver fibrosis. Hepatology.
17. Venugopal SK, Jiang J, Kim TH, Li Y, Wang SS, et al. (2010) Liver fibrosis causes downregulation of miRNA-150 and miRNA-194 in hepatic stellate cells, and their overexpression causes decreased stellate cell activation. Am J Physiol Gastrointest Liver Physiol 298: G101–106.
18. Jiang J, Gusev Y, Aderca I, Mettler TA, Nagorney DM, et al. (2008) Association of MicroRNA expression in hepatocellular carcinomas with hepatitis infection, cirrhosis, and patient survival. Clin Cancer Res 14: 419–427.
19. Jiang X, Tsitsiou E, Herrick SE, Lindsay MA (2010) MicroRNAs and the regulation of fibrosis. Febs J 277: 2015–2021.
20. Marquez RT, Bandyopadhyay S, Wendlandt EB, Keck K, Hoffer BA, et al. (2010) Correlation between microRNA expression levels and clinical parameters associated with chronic hepatitis C viral infection in humans. Lab Invest.
21. Kim S, Lee UJ, Kim MN, Lee EJ, Kim JY, et al. (2008) MicroRNA miR-199a* regulates the MET proto-oncogene and the downstream extracellular signal-regulated kinase 2 (ERK2). J Biol Chem 283: 18158–18166.
22. Murakami Y, Aly HH, Tajima A, Inoue I, Shimotohno K (2009) Regulation of the hepatitis C virus genome replication by miR-199a. J Hepatol 50: 453–460.
23. Gibbons DL, Lin W, Creighton CJ, Rizvi ZH, Gregory PA, et al. (2009) Contextual extracellular cues promote tumor cell EMT and metastasis by regulating miR-200 family expression. Genes Dev 23: 2140–2151.
24. Gregory PA, Bert AG, Paterson EL, Barry SC, Tsykin A, et al. (2008) The miR-200 family and miR-205 regulate epithelial to mesenchymal transition by targeting ZEB1 and SIP1. Nat Cell Biol 10: 593–601.
25. Oberti F, Valsesia E, Pilette C, Rousselet MC, Bedossa P, et al. (1997) Noninvasive diagnosis of hepatic fibrosis or cirrhosis. Gastroenterology 113: 1609–1616.
26. Xu L, Hui AY, Albanis E, Arthur MJ, O'Byrne SM, et al. (2005) Human hepatic stellate cell lines, LX-1 and LX-2: new tools for analysis of hepatic fibrosis. Gut 54: 142–151.
27. Aly HH, Watashi K, Hijikata M, Kaneko H, Takada Y, et al. (2007) Serum-derived hepatitis C virus infectivity in interferon regulatory factor-7-suppressed human primary hepatocytes. J Hepatol 46: 26–36.

Murakami et al. BMC Medical Genomics 2010, 3:48
http://www.biomedcentral.com/1755-8794/3/48

BMC Medical Genomics

RESEARCH ARTICLE Open Access

Hepatic microRNA expression is associated with the response to interferon treatment of chronic hepatitis C

Yoshiki Murakami[1*], Masami Tanaka[2], Hidenori Toyoda[3], Katsuyuki Hayashi[4], Masahiko Kuroda[2], Atsushi Tajima[5], Kunitada Shimotohno[6]

Abstract

Background: HCV infection frequently induces chronic liver diseases. The current standard treatment for chronic hepatitis (CH) C combines pegylated interferon (IFN) and ribavirin, and is less than ideal due to undesirable effects. MicroRNAs (miRNAs) are endogenous small non-coding RNAs that control gene expression by degrading or suppressing the translation of target mRNAs. In this study we administered the standard combination treatment to CHC patients. We then examined their miRNA expression profiles in order to identify the miRNAs that were associated with each patient's drug response.

Methods: 99 CHC patients with no anti-viral therapy history were enrolled. The expression level of 470 mature miRNAs found their biopsy specimen, obtained prior to the combination therapy, were quantified using microarray analysis. The miRNA expression pattern was classified based on the final virological response to the combination therapy. Monte Carlo Cross Validation (MCCV) was used to validate the outcome of the prediction based on the miRNA expression profile.

Results: We found that the expression level of 9 miRNAs were significantly different in the sustained virological response (SVR) and non-responder (NR) groups. MCCV revealed an accuracy, sensitivity, and specificity of 70.5%, 76.5% and 63.3% in SVR and non-SVR and 70.0%, 67.5%, and 73.7% in relapse (R) and NR, respectively.

Conclusions: The hepatic miRNA expression pattern that exists in CHC patients before combination therapy is associated with their therapeutic outcome. This information can be utilized as a novel biomarker to predict drug response and can also be applied to developing novel anti-viral therapy for CHC patients.

Background

Hepatitis C virus (HCV) infection affects more than 3% of the world population. HCV infection frequently induces chronic liver diseases ranging from chronic hepatitis (CH) C, to liver cirrhosis (LC) and hepatocellular carcinoma (HCC) [1]. The current standard treatment for CHC combines pegylated interferon (Peg-IFN) and ribavirin, and has been found to be effective in only 50% of HCV genotype 1b infection. Furthermore this form of therapy is often accompanied by adverse effects; therefore, there is a pressing need to develop alternative strategies to treat CHC and to identify patients that will not be responsive to treatment [2].

MicroRNAs (miRNAs) are endogenous small non-coding RNAs that control gene expression by degrading or suppressing the translation of target mRNAs [3,4]. There are currently 940 identifiable human miRNAs (The miRBase Sequence Database – Release 15.0). These miRNAs can recognize hundreds of target genes with incomplete complementary over one third of human genes appear to be conserved miRNA targets [5,6]. miRNA can associate not only several pathophysiologic events but also cell proliferation and differentiation.

However, there are many miRNAs whose functions are still unclear. Examples include miR-122 which is an abundant liver-specific miRNA that is said to constitute

* Correspondence: ymurakami@genome.med.kyoto-u.ac.jp
[1]Center for Genomic Medicine, Kyoto University Graduate School of Medicine, 53 Shogoinkawahara-cho, Sakyo-ku, Kyoto 606-8507, Japan
Full list of author information is available at the end of the article

up to 70% of all miRNA molecules in hepatocytes [7]. The expression level of miR-122 was reportedly associated with early response to IFN treatment, while others like miR-26 have expression status that is associated with HCC survival and response to adjuvant therapy with IFN [8,9]. IFN beta (IFNβ) on the other hand, has been shown to rapidly modulate the expression of numerous cellular miRNAs, and it has been demonstrated that 8 IFNβ-induced miRNAs have sequence-predicted targets within the hepatitis C virus (HCV) genomic RNA [10]. Finally several miRNAs have been recognized as having target sites in the HCV genome that inhibits viral replication [10-12].

To date, various parameters have been examined in an attempt to confirm the effects of the IFN-related treatment for CHC. In patients with chronic HCV genotype 1b infection, there is a substantial correlation between responses to IFN and mutation in the interferon sensitivity determining region (ISDR) of the viral genome [13]. Substitutions of amino acid in the HCV core region (aa 70 and aa 91) were identified as predictors of early HCV-RNA negativity and several virological responses, including sustained response to standard combination therapy [14]. In order to assess the drug response to combination therapy for CHC using gene expression signatures, several researchers cataloged the IFN related gene expression profile from liver tissue or peripheral blood mononuclear cells (PBMC) [15,16]. It was found that failed combination therapy was associated with up-regulation of a specific set of IFN-responsive genes in the liver before treatment [17]. Additional reports have indicated that two SNPs near the gene IL28B on chromosome 19 may also be associated with a patient's lack of response to combination therapy [18]. These reports suggest that gene expression during the early phase of anti-HCV therapy may elucidate important molecular pathways for achieving virological response [19].

Our aim in this study was to identify gene related factors that contribute to poor treatment response to combination therapy for CHC. In order to achieve this we studied the miRNA expression profile of CHC patients before treatment with CHC combination therapy and tried to determine the miRNAs that were associated with their drug response. Knowing patients' expression profile is expected to provide a clearer understanding of how aberrant expression of miRNAs can contribute to the development of chronic liver disease as well as aid in the development of more effective and safer therapeutic strategies for CHC.

Methods

Patients and sample preparation

Ninety-nine CHC patients with HCV genotype 1b were enrolled (Table 1). Patients with autoimmune hepatitis, or alcohol-induced liver injury, or hepatitis B virus-associated antigen/antibody or anti-human immunodeficiency virus antibody were excluded. There were no patients who received IFN therapy or immunomodulatory therapy before enrollment in the study. Serum HCV RNA was quantified before IFN treatment using Amplicor-HCV Monitor Assay (Roche Molecular Diagnostics Co., Tokyo, Japan). Liver biopsy specimen was collected from each patient up to one week prior to administering combination therapy. Histological grading and staging of liver biopsy specimens from the CHC patients were performed according to the Metavir classification system. Pretreatment blood tests were conducted to determine each patient's level of aspartate aminotransferase, alanine aminotransferase, total bilirubin, alkaline phosphatase, gamma-glutamyl transpeptidase, white blood cell (WBC), platelets, and hemoglobin. Written informed consent was obtained from all of the patients or their guardians and provided to the Ethics Committee of the Graduate School of Kyoto University, who approved the conduct of this study in accordance with the Helsinki Declaration.

Table 1 Clinical characteristics of patients

Characteristics	SVR (n = 46)	R (n = 28)	NR (n = 25)	p-value
Age (years)	57.0 ± 9.8	61.2 ± 8.3	60.6 ± 7.6	0.09†
Male (%)	28 (61%)	11 (39%)	9 (36%)	0.08§
Weight (kg)	59.5 ± 9.0	56.6 ± 9.9	56.0 ± 7.7	0.13†
HCV RNA ($\times 10^6$ copies/ml)	1.90 ± 1.95	1.83 ± 1.04	1.58 ± 0.93	0.62†
Fibrosis stage				
F 0	1	1	1	0.50§
F 1	29	16	10	
F 2	10	7	6	
F 3	6	4	7	
F 4	0	0	1	
WBC($\times 10^3/mm^3$)	5.31 ± 1.59	5.18 ± 1.24	4.71 ± 1.15	0.29†
Hemoglobin (g/dl)	14.2 ± 1.26	13.6 ± 1.35	13.5 ± 1.13	0.022†
Platelet ($\times 10^4/mm^3$)	16.7 ± 5.0	16.4 ± 4.0	15.2 ± 6.1	0.25†
AST (IU/L)	54.8 ± 48.1	46.6 ± 29.3	57.0 ± 28.5	0.17†
ALT (IU/L)	74.5 ± 87.8	47.9 ± 28.6	67.6 ± 43.2	0.15†
γGTP (IU/L)	56.0 ± 69.4	38.5 ± 28.9	74.3 ± 59.0	0.025†
ALP (IU/L)	248 ± 71.5	245 ± 75.7	323 ± 151	0.038†
Total Bilirubin (mg/dl)	0.67 ± 0.22	0.72 ± 0.30	0.68 ± 0.19	0.95†
Albumin (g/dl)	4.21 ± 0.31	4.13 ± 0.27	4.01 ± 0.48	0.14†

Abbreviations. SVR, sustained virological response; R, relapse; NR, non responder; Differences in clinical characteristics among three groups were tested using †Kruskal-Wallis test, or §Fisher's exact test. AST, aspartate aminotransferase; ALT, alanine aminotransferase; WBC, white blood cell; ALP, alkaline phosphatase; γGTP, gamma-glutamyl transpeptidase.

Treatment protocol and definitions

All enrolled patients were treated with pegylated IFNa-2b (Schering-Plough Corporation, Kenilworth, NJ, USA) and ribavirin (Schering-Plough) for 48 weeks (Figure 1). Pegylated IFN was administered at a dose of 1.5 mg kg/week at the starting point. Ribavirin was administered following the dose recommended by the manufacturer.

Definitions of drug response to therapy

Drug response was defined according to how much HCV RNA had decreased in each patient's serum. After four weeks of drug administration (rapid response phase) the patients were classified into the following two groups after four weeks of drug administration: (i) rapid virological responder (RVR): a patient whose serum was negative for serum HCV RNA at four weeks, and (ii) non-RVR: a patient who was not classified as RVR.

The patients were classified into the following three groups after 12 weeks of drug administration (early response phase): (i) complete early virological responder (cEVR): a patient who was negative for serum HCV RNA at 12 weeks; (ii) partial EVR: a patient whose serum HCV RNA was reduced by 2-log or more of the HCV RNA before drug administration at 12 weeks, but who was not negative for serum HCV RNA; and (iii) non-EVR: a patient who was not classified as either cEVR or pEVR.

The patients were classified into the following three groups at the time of post-treatment at 24 weeks (final response): (i) sustained virological responder (SVR): a patient who was negative for serum HCV RNA during the six months following completion of the combination therapy; (ii) relapse (R): a patient whose serum HCV RNA was negative by the end of the combination therapy but reappeared after completion of the combination therapy; and (iii) virological non-responder (NR): a patient who was positive for serum HCV RNA during the entire course of the combination treatment.

RNA extraction

Liver biopsy specimens were stored in RNA later (Ambion, Austin, TX, USA) at -80°C until RNA

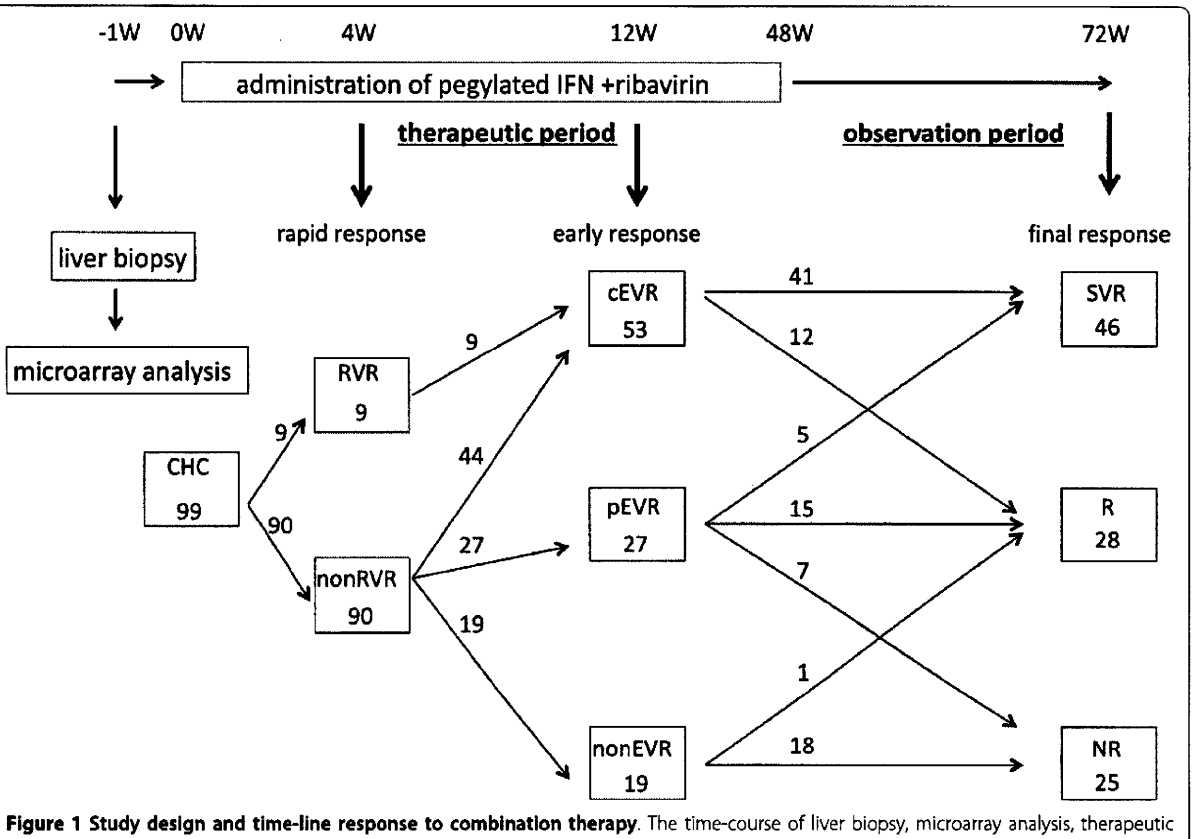

Figure 1 Study design and time-line response to combination therapy. The time-course of liver biopsy, microarray analysis, therapeutic period, observation period after combination therapy, and drug response judgment time (4W, 12W, 72W) is shown. Each therapeutic result (rapid, early, and final response) and the number of patients transitioning into each group are shown. RVR, cEVR, pEVR, SVR, R, and NR are denoted as rapid virological response, complete early virological response, partial EVR, sustained virological response, relapse, and non responder, respectively.

extraction. Total RNA was extracted by using mirVana™ miRNA Isolation kit (Ambion) according to the manufacturer's instruction.

miRNA microarray

miRNA microarrays were manufactured by using Agilent Technologies (Santa Clara, CA, USA). Total RNA (100 ng) were labeled and hybridized using a Human microRNA Microarray kit (Agilent Technologies) according to the manufacturer's protocol (Protocol for use with Agilent microRNA microarrays Version 1.5). Hybridization signals were detected using the DNA microarray scanner G2505B (Agilent Technologies), and all scanned images were analyzed using Agilent feature extraction software (v9.5.3.1). Data were analyzed using GeneSpring GX 7.3.1 software (Agilent Technologies) and normalized as follows: (i) values below 0.01 were set to 0.01. (ii) each measurement was divided by the 75th percentile of all measurements to compare one-color expression profiles. The data presented in this manuscript have been deposited in NCBI's Gene Expression Omnibus and are accessible through GEO Series accession number GSE16922: http://www.ncbi.nlm.nih.gov/geo/query/acc.cgi?token=xlmbxyyumcwkeba&acc=GSE16922

Real-time qPCR for miRNA quantification

To detect the expression level of miRNA by real-time qPCR, TaqMan® microRNA assay (Applied Biosystems) was used to quantify the relative expression levels of miR-18a (assay ID, 002422), miR-27b (assay ID, 000409), miR-422b (assay ID, 000575), miR-143 (assay ID, 000466), miR-145 (assay ID, 000467), miR-34b (assay ID, 000427), miR-378 (assay ID, 000567) and U18 (assay ID, 001204) which was used as an internal control. cDNA was synthesized by Taqman miRNA RT Kit (Applied Biosystems). Total RNA (10 ng) in 5 ul of nuclease free water was added to 3 ul of 5× RT primer, 10× 1.5 ul of reverse transcriptase buffer, 0.15 ul of 100 mM dNTP, 0.19 ul of RNase inhibitor, 4.16 ul of nuclease free water, and 50 U of reverse transcriptase in a total volume of 15 ul. The reaction was performed for 30 min at 16°C, 30 min at 42°C, and five min at 85°C. All RT reactions were run in triplicate. Chromo 4 detector (BIO-RAD, Hercules, CA, USA) was used to detect miRNA expression.

Method of predicting prognosis

Monte Carlo Cross Validation (MCCV) was used to identify a set of prognostic miRNAs and to assess and predict drug response [20,21]. We chose MCCV to make up for relatively small number of patients. The 99 enrolled patients were repeatedly and randomly divided 100 times into training sets (TSs; size n = 10, 20, ..., 90) and a corresponding validation set (VS; size = 99-n). The percentile-normalized measures for miRNA expression were compared between the 2 TS patient groups of SVR and non-SVR (R and NR) by computing absolute values of the difference for each of the 172 miRNAs that were higher than 10. A prognosis signature was defined in terms of the expression measures of the miRNAs with the largest absolute differences. A 35-miRNA prognosis predictor (PP) was established for TS patients and its performance was assessed on VS patients. A PP was computed by applying diagonal linear discriminant analysis to the 35-miRNA PP of the TS patients (Table 2 and 3). The PP was applied to predict the prognoses of the VS patients. The predicted and actual prognoses (SVR or non-SVR) of the VS patients were compared to obtain the following three measures of prognosis prediction performance: (1) accuracy (proportion of correctly predicted prognoses), (2) sensitivity (proportion of correctly predicted non-SVR) and (3) specificity (proportion of correctly predicted SVR). 53 patients (N and NR) were also repeatedly and randomly divided 100 times into training sets (TSs; size n = 6, 12, ...42) and corresponding validation set (VS; size = 53-n). Perl programs of our own writing performed all analytical processes.

Cell lines and miRNA transfection

HEK293 cells were maintained in D-MEM (Invitrogen, Carlsbad, CA, USA) with 10% fetal bovine serum, plated in 60 mm diameter dishes and cultured to 70% confluence. 293 cells were plated in 6-well plates the day before transfection and grown to 70% confluence. Cells were transfected with 50 pmol of Silencer® negative control siRNA (Ambion) or double-stranded mature miRNA (ds miRNA) or 2'-O-methylated antisense oligonucleotide against the miRNA of interest (ASO miRNA) (Hokkaido System Science, Sapporo, Japan) using lipofectamine RNAiMAX (Invitrogen). Cells were harvested 2 days after transfection.

Real-time qPCR for mRNA quanification

cDNA was synthesized using the Transcriptor High Fiderity cDNA synthesis Kit (Roche, Basel, Switzerland). Total RNA (2 μg) in 10.4 μl of nuclease free water was added to 1 μl of 50 mM random hexamer. The denaturing reaction was performed for 10 min at 65°C. The denatured RNA mixture was added to 4 μl of 5× reverse transcriptase buffer, 2 μl of 10 mM dNTP, 0.5 μl of 40 U/μl RNase inhibitor, and 1.1 μl of reverse transcriptase (FastStart Universal SYBR Green Master (Roche) in a total volume of 20 μl. The reaction ran for 30 min at 50°C (cDNA synthesis), and five min at 85°C (enzyme denaturation). All reactions were run in triplicate. Chromo 4 detector (BIO-RAD, Hercules, CA, USA) was used to detect mRNA expression. The primer sequences are as follows; BCL2 s; 5'-gttgctttacgtggcctgtt-3', as; 5'-ggaggtctggcttcatacca-3', RARA s; 5'-cataccctgccataccaacc-

Table 2 List of the 35 miRNAs used to classify patients into SVR and non-SVR groups using Monte Carlo Cross Validation (MCCV)

Gene name	fold change (SVR/non SVR)	T-test	Selection by MCCV		
			Rank	appearance frequency in this classification (%)	appearance number of times
hsa-miR-122a	1.32	6.67E-02	1	98.78	889
hsa-miR-21	1.19	3.62E-01	2	94.67	852
hsa-miR-22	1.23	7.80E-02	3	93.22	839
hsa-let-7a	1.14	3.57E-01	4	92.33	831
hsa-miR-23b	1.41	1.72E-02	5	91.44	823
hsa-miR-26a	1.32	7.45E-02	6	90.78	817
hsa-let-7f	1.15	4.04E-01	7	88.67	798
hsa-miR-142-3p	1.39	1.45E-01	8	87.33	786
hsa-miR-494	2.18	5.85E-03	9	82.00	738
hsa-miR-194	1.22	1.70E-01	10	80.78	727
hsa-let-7b	1.11	3.59E-01	11	80.22	722
hsa-miR-148a	1.25	2.28E-01	12	79.67	717
hsa-miR-29a	1.16	2.73E-01	13	77.78	700
hsa-miR-125b	1.20	2.37E-01	14	73.11	658
hsa-miR-192	1.09	4.89E-01	15	69.67	627
hsa-miR-24	1.25	8.31E-02	16	68.89	620
hsa-miR-768-3p	1.19	1.78E-01	17	68.78	619
hsa-miR-126	1.07	6.75E-01	18	49.56	446
hsa-miR-19b	1.15	2.98E-01	19	48.89	440
hsa-miR-370	2.00	1.44E-02	20	39.00	351
hsa-miR-29c	1.26	1.37E-01	21	38.89	350
hsa-miR-16	1.24	2.08E-01	22	37.11	334
hsa-miR-145	1.01	9.25E-01	23	34.89	314
hsa-let-7c	1.21	1.41E-01	24	33.22	299
hsa-miR-215	1.20	3.65E-01	25	27.67	249
hsa-let-7g	1.16	3.64E-01	26	27.44	247
hsa-miR-451	1.13	6.94E-01	27	23.11	208
hsa-miR-26b	1.30	2.26E-01	28	22.22	200
hsa-miR-92	1.12	3.44E-01	29	21.11	190
hsa-miR-29b	1.19	2.62E-01	30	19.44	175
hsa-miR-107	1.21	1.58E-01	31	18.78	169
hsa-miR-27b	1.40	2.32E-02	32	18.11	163
hsa-miR-638	1.32	5.57E-02	33	16.89	152
hsa-miR-199a*	1.12	5.92E-01	34	16.78	151
hsa-miR-193b	1.25	7.24E-02	35	16.67	150

3', as; 5'-gacatgaaaggagagtgggg-3', SMAD2 s; 5'-aatattttgg ggactgatgcc-3', as; 5'-gcttttgggcagtggttaag-3', and β-actin s; 5'-ccactggcatcgtgatggac-3', as; 5'-tcattgccaatggtgat-gacct-3'. Assays were performed in triplicate, and the expression levels of target genes were normalized to the expression of the β-actin gene, as quantified using real-time qPCR as internal controls.

Statistical analysis

Data were statistically analyzed using the Student's t-test and differences in clinical characteristics among 3 groups were tested using the Kruskal-Wallis test, or Fisher's exact test. Data from microarray were also statically analyzed using Welch's test and Benjamini-Hochberg correction for multiple hypotheses testing.

Results

A microarray platform was used to determine miRNA expression of 470 miRNAs in 99 fresh-frozen CHC liver tissues.

miRNAs which related to the final response of combination therapy

Unique miRNA expression patterns were established according to the final virological response (SVR, R, and NR) to the combination therapy (Figure 1). To isolate